

# Research on Layer-Subdivision of Artificial Edge-Water Flooding in Low-Amplitude Structural Medium-Permeability Reservoirs<sup>#</sup>

Jiqiang Wu<sup>1</sup>, Shijun Huang<sup>1</sup>, Miaomiao Liu<sup>1</sup>, Wenxuan Gao<sup>1</sup>, Shuang Zhang<sup>2</sup>, Yang Wang<sup>3</sup>

1 China University of Petroleum (Beijing)

2 PetroChina Liaohe Oilfield Company

3 Qingdao University of Technology

(Corresponding Author: gushiqiye3@qq.com)

## ABSTRACT

The concept of low-amplitude structures, also known as micro-amplitude structures and micro-structures, generally refers to reservoirs with an oil-bearing height of less than 10m. Low-amplitude structures are generally likely to obtain industrial oil flows and have good exploration prospects. Artificial edge-water flooding, recently developed by Shengli Oilfield, serves as a water flooding alternative for enhancing oil recovery in complex fault-block reservoirs during the ultra-high water-cut stage. While this technology has demonstrated favorable field application results, its efficacy in low-amplitude structural reservoirs warrants further investigation. The C1 Block in Shengli Oilfield has long vertical oil-bearing well sections, multiple layered systems, and low structural amplitude. This study employs theoretical analysis, numerical simulation, and dynamic performance evaluation to examine artificial edge-water flooding in the medium-permeability, low-amplitude reservoir of the C1 Block. The findings reveal that low-amplitude structures exert significant control over the original distribution and enrichment of oil and water. A multi-factor indicator system was applied to subdivide the reservoir vertically into four distinct layer series for development. Investigations into influencing factors of the artificial edge-water flooding process have identified key directions for future reservoir management strategies.

**Keywords:** Low-Amplitude Structures, Artificial Edge-Water Flooding, Layer-Subdivision, Multi-factor Index

## NONMENCLATURE

### Abbreviations

AHP Analytic Hierarchy Process

### Symbols

n Year

## 1. INTRODUCTION

Low-amplitude structures are geological bodies characterized by low structural closure, typically with amplitudes of only 10–20 meters. Structural and sedimentary studies indicate that the formation of low-relief structures is often controlled by depression locations and major faults. From the perspective of hydrocarbon accumulation, the faults intersecting low-relief structures are generally minor, making it difficult for them to directly connect with source rocks or other reservoirs. Consequently, vertical hydrocarbon migration is limited, and lateral migration represents the primary mechanism for hydrocarbon sourcing. A typical migration model involves hydrocarbons moving upward from deeper sections through fault systems into carrier beds, followed by lateral migration within these beds, ultimately accumulating in low-amplitude structural traps. Such structures often yield commercial hydrocarbon flows and demonstrate promising exploration potential<sup>[1-3]</sup>. Microstructures of oil layers are defined as "structural features reflected by subtle undulations of the reservoir itself within the broader structural framework of the oilfield," generally covering an area of less than 0.3 km<sup>2</sup> with relief not exceeding 20 meters. In recent years, research on low-amplitude structures has continued to evolve, covering a wide range of oilfields and regions, with adjustments in the amplitude criteria. However, the technical approach remains primarily focused on detailed processing and interpretation of seismic data<sup>[4-7]</sup>.

Artificial edge water flooding is a water technology proposed in the Shengli Oil Field in recent years. This technique involves large-well-spacing, high-rate water injection at the structurally low parts of complex fault-block reservoirs to simulate strong natural edge water drive, thereby improving development performance. For complex fault-block reservoirs in the ultra-high water-cut stage, the "inject-before-produce" approach can

<sup>#</sup> This is a paper for the 17th International Conference on Applied Energy (ICAE2025), December 8-12, 2025, Bangkok, Thailand.

promote the redistribution and reaccumulating of highly dispersed remaining oil toward structural highs, effectively enhancing oil recovery<sup>[8-13]</sup>. Therefore, this study integrates theoretical analysis, numerical simulation, and performance analysis to investigate imitation edge water flooding in the layered, medium-permeability reservoir of the C1 Block with low-amplitude structures. It was found that these structures exert strong control over the distribution and enrichment of original oil and water. A development strategy involving the vertical subdivision of four-layer series based on a multi-factor index system was adopted. Research on factors influencing the imitation edge water flooding clarified the direction for later-stage reservoir adjustment.

## 2. RESERVOIR OVERVIEW AND STRUCTURAL CHARACTERISTICS

### 2.1 Reservoir Overview

The stratigraphic thickness of C1 Block ranges from approximately 200 to 480 meters, primarily composed of interbedded light gray siltstone, fine sandstone, and green-gray mudstone in varying thicknesses, with intercalations of gray calcareous sandstone, calcareous siltstone, calcareous mudstone, argillaceous siltstone, and silty mudstone.

Based on current development requirements, guided by marker beds and applying cyclic correlation and hierarchical control methods, the sand layers have been divided into 8 sand groups and 37 sub-layers, among which 32 contain oil. Core physical property analysis indicates that the porosity ranges from a maximum of 29.2% to a minimum of 12.9%, with an average value of 24%. The permeability ranges from a maximum of  $2214 \times 10^{-3} \mu\text{m}^2$  to a minimum of  $20 \times 10^{-3} \mu\text{m}^2$ , with an average of  $305 \times 10^{-3} \mu\text{m}^2$ . This characterizes the reservoir as having moderate porosity and permeability.

### 2.2 Low-Relief Structural Characteristics

The C1 Block exhibits an overall monoclinic structure dipping northward, characterized by a gentler southern flank and a steeper northern slope, with structural dip angles ranging from  $6^\circ$  to  $9^\circ$ . Based on fault assemblage characteristics, the study area can be subdivided into four microstructural zones (Fig.1). The Northern Monocline Zone displays relatively subdued structural relief, maintaining a simple north-dipping monoclinic configuration. Two minor nose-like structures with low structural relief are developed within this zone. In the C1

Anticlinal Structural Zone, localized south-dipping strata occur within the regional northeast-dipping background, forming an elongated east-west trending anticline. The southern limb dips at approximately  $4^\circ$ , while the northern limb exhibits a dip angle of about  $3^\circ$ . The C41 Fault-Nose Structural Zone primarily developed through tilting of the uplifted fault block. At the top surface of the Es<sub>2</sub><sup>1</sup> sub-member, this zone manifests as a weakly south-dipping nose-like structure. Although the central portion of this fault-nose structure is disrupted by two minor faults, its overall configuration remains clearly identifiable, representing a potentially effective structural trap. However, longitudinal analysis indicates that the south-dipping attitude of this fault-nose diminishes rapidly and becomes essentially unrecognizable within the Es<sub>2</sub><sup>3</sup> sand group. The Southern Monocline Zone largely reverts to the regional north-dipping monoclinic structural pattern.

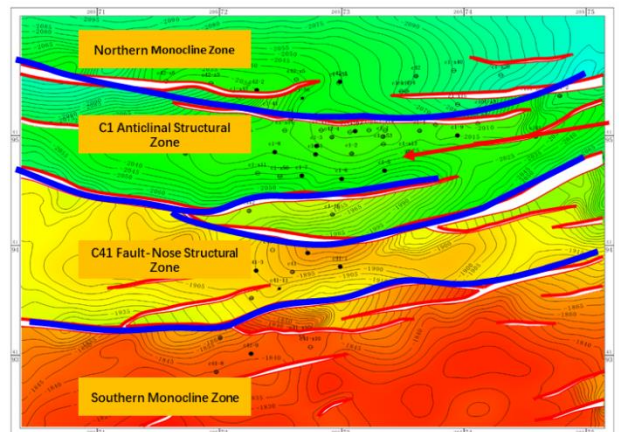


Fig. 1 Schematic Diagram of Structural Zonation in the C1 Block

Utilizing data from 61 wells in the C1 Block, microstructural maps were generated for the top surfaces of 27 sub-layers within the eight sand groups of the Sha-2 Member (Fig.2-3). These maps reveal that, against the overall structural background, each sub-layer exhibits local micro-scale undulations characterized by small amplitude and limited areal extent, with relative relief generally ranging between 1 and 5 meters.

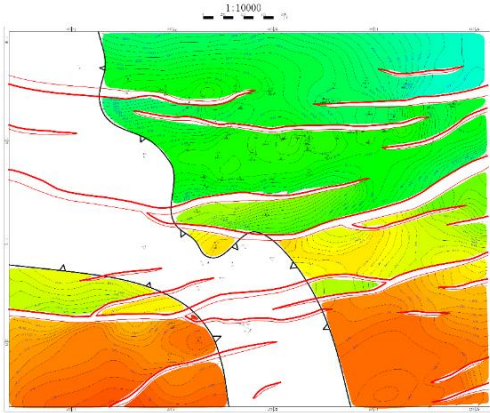


Fig2. Microstructural Map of the Top Surface of  $Es_2^{1^1}$  Sand Body

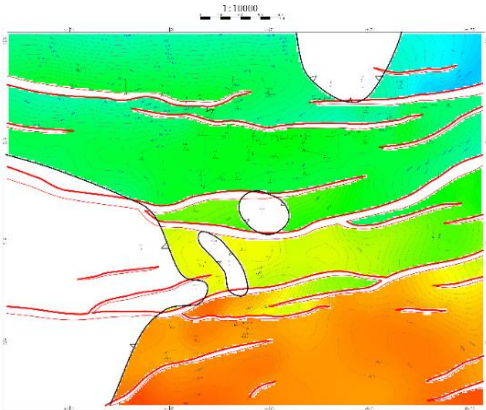


Fig3. Microstructural Map of the Top Surface of  $Es_2^1$  Sand Body

### 3. CONTROL EFFECTS OF LOW-AMPLITUDE STRUCTURES ON DEVELOPMENT DYNAMICS

The C1 Block exhibits multiple oil-water systems. Different sub-layers possess distinct oil-water contacts (OWCs), and even within the same sub-layer, various oil-bearing sand bodies show differing OWCs. The average ground oil density is  $0.8869 \text{ g/cm}^3$ , with an oil-water density difference of  $0.1131 \text{ g/cm}^3$ . The average ground viscosity is  $53.2 \text{ mPa}\cdot\text{s}$ . These variations indicate that the reservoir possesses the fundamental conditions necessary for hydrocarbon-water differentiation and directional migration. The initial water cut is a function of the initial water saturation. A lower initial water saturation corresponds to a lower initial water cut and higher initial oil productivity. In other words, the initial water cut can reflect the original oil saturation and the degree of hydrocarbon accumulation. Therefore, investigating the relationship between low-amplitude structures and well productivity can effectively reveal the extent to which these structures control and influence the distribution and enrichment of oil and water within the C1 Block reservoir.

Based on production test data, both initial stable production rates and initial water cut were observed to closely follow the subtle undulations and natural extensions of the low-amplitude structures. Areas with higher structural relief generally exhibit higher initial daily oil production capacity, lower water cut, and greater net pay thickness. Conversely, zones with lower structural relief are characterized by lower initial daily oil production capacity, higher water cut, and reduced net pay thickness. Furthermore, the spatial influence of these structural configurations is scale-dependent. Larger structural assemblages exert control over broader areas, while smaller assemblages have more localized effects. These findings demonstrate that low-amplitude structures and their spatial scale play a significant role in controlling the original distribution and enrichment of oil, gas, and water in medium- to high-permeability reservoirs (Fig.4).

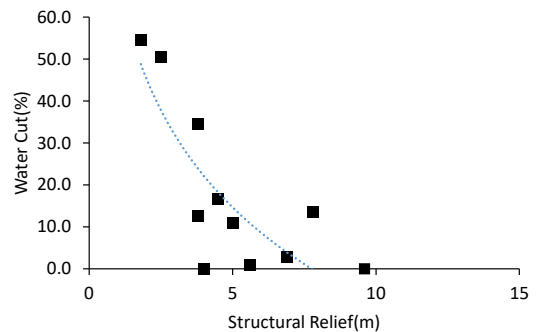
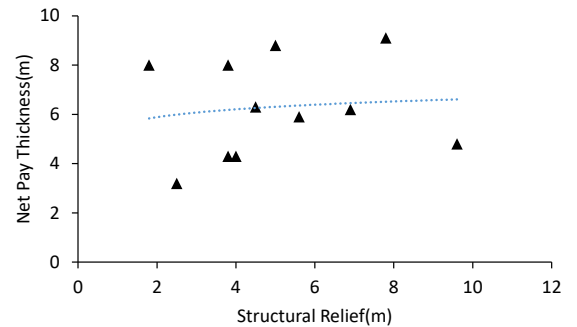
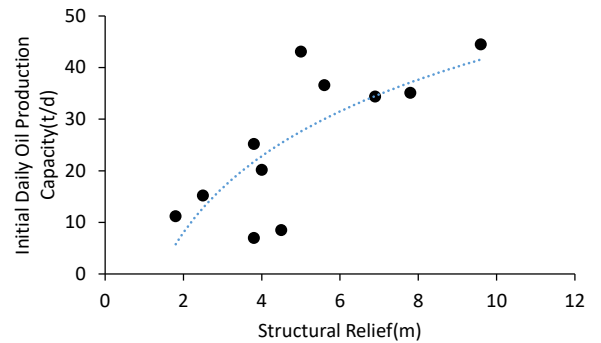


Fig4. Relationship Between Structural Relief and Reservoir Parameters

#### 4. COMPREHENSIVE EVALUATION METHOD FOR MULTI-LAYER RESERVOIR CLASSIFICATION

##### 4.1 Necessity of Layer Series Subdivision

The C1 Block reservoir is currently developed using a single-layer system, characterized by high reserve abundance and substantial reserves controlled per well. The reserve abundance of the block reaches  $113.8 \times 10^4$  t/km<sup>2</sup>, with reserves controlled per well amounting to  $11.0 \times 10^4$  t. Among its sub-areas, the C1 well area covers the largest extent, containing 23 oil-bearing sub-layers, including 8 major oil-bearing sub-layers, and exhibits a reserve abundance of  $166.8 \times 10^4$  t/km<sup>2</sup>. Taking the C1 well area as an example, significant variations exist in the oil-bearing area across different layers. The main layer, Es2<sup>31</sup>, has an oil-bearing area of 0.62 km<sup>2</sup>, while the non-main layer, Es2<sup>87</sup>, has a minimal oil-bearing area of only 0.07 km<sup>2</sup>. The current single-layer development strategy is unable to effectively address the production needs of both the main and non-main layers simultaneously (Fig.5).

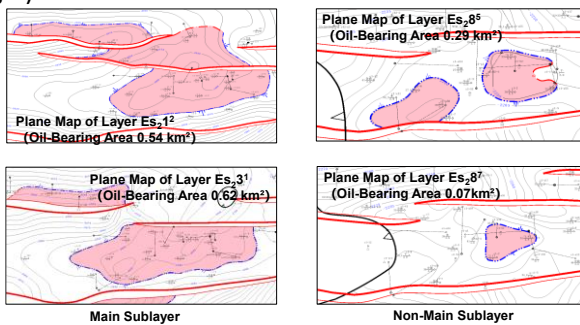


Fig5. Plane Map of Sublayers in the Main Block of C1

Currently, in the C1 Block, commingled production in some wells has intensified interlayer interference, negatively impacting well productivity. A correlation analysis between the perforated thickness and oil production intensity during the initial production period indicates that as the perforated thickness increases, the oil production intensity decreases. Significant disparities exist in reserve scale and recovery degree among different layers. The main layers, with larger reserves, exhibit higher recovery degrees, whereas the non-main layers, with smaller reserves, show lower recovery degrees. Under the current single-layer development strategy, water injection profiles are highly imbalanced across sub-layers, with substantial interlayer heterogeneity. Main layers absorb significantly more injected water than non-main layers (Fig.6). For instance, in well C1-2, the sub-layer Es2<sup>85</sup> has the highest relative water absorption at 23.1%, while sub-layer Es2<sup>32</sup> has the lowest, at only 3.8%.

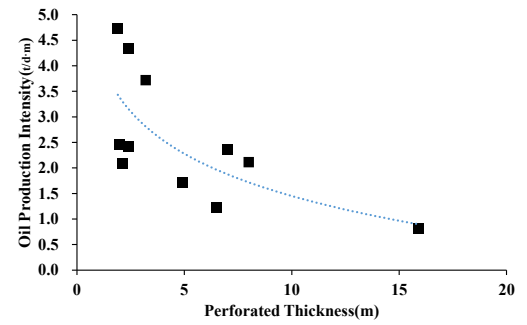


Fig6. Correlation Curve Between Oil Production Intensity and Perforated Thickness

##### 4.2 Construction and Classification of a Development Index System for Multi-Layer Reservoirs

After long-term water flooding development in blocks such as C1, it is difficult to evaluate the potential for flow field adjustment using a single parameter. Therefore, a comprehensive evaluation method incorporating multiple static and dynamic development parameters should be applied to conduct a quantitative assessment of the field's development potential. It is essential to comprehensively consider principles such as material basis, controlling factors and evaluation parameters. The selected indicators should exhibit strong independence and be readily obtainable from production data or reservoir models.

After selecting the evaluation indicators, it is necessary to define the hierarchical structure of these indicators, organizing them into multiple tiers based on their attributes and interrelationships (Fig.7). The first-level indicators, also referred to as the criterion layer, include Material Basis, Controlling Factors, and Development Potential. Each first-level indicator is further subdivided into second-level indicators: Material Basis comprises three second-level indicators: reserves, area, and formation coefficient; Controlling Factors includes two second-level indicators: well pattern control degree and edge water energy; Development Potential consists of two second-level indicators: remaining reserves and water cut. Indicators at higher levels exert a governing influence over those at lower levels. The scaling of these indicators is performed in accordance with the standard methodology of Analytic Hierarchy Process (AHP), as specified in Table 1.

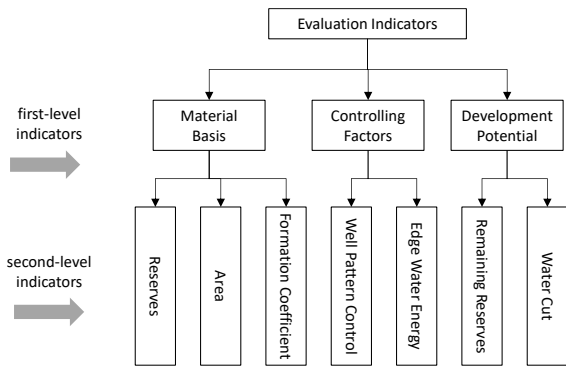


Fig7. Comprehensive Evaluation Index System

Table 1. Analytic Hierarchy Process (AHP) Scale Table

AHP Judgment Scale	Its Semantic Interpretations
1	Equal importance — Two factors contribute equally to the objective.
3	Moderate importance — One factor is slightly more important than the other.
5	strong importance — One factor is significantly more important than the other.
7	Very strong importance — One factor is strongly favored over the other.
9	Extreme importance — The dominance of one factor over the other is affirmed with the highest certainty.
2,4,6,8	Intermediate values — Used to represent compromises between adjacent levels of importance.
Reciprocal Rule:	If the comparison of element $A_i$ with $A_j$ yields a scale value $a_{ij}$ , then the comparison of $A_j$ with $A_i$ is represented by the reciprocal value $a_{ji}=1/a_{ij}$ .

Using the Analytic Hierarchy Process (AHP), a pairwise comparison was first conducted among the first-level indicators within the evaluation system. The comparative analysis focused on the three primary criteria: Material Basis, Controlling Factors, and Development Potential. The resulting judgment matrix

for these first-level indicators is 
$$\begin{bmatrix} 1 & 5 & 7 \\ \frac{1}{5} & 1 & 3 \\ \frac{1}{7} & \frac{1}{3} & 1 \end{bmatrix}$$
, yielded

the following weight vector (0.730,0.189,0.081).

For the second-level indicators within the Material Basis criterion (Reserves, Area, and Formation Coefficient), the pairwise comparison matrix is

constructed as follows 
$$\begin{bmatrix} 1 & 3 & 5 \\ \frac{1}{3} & 1 & 3 \\ \frac{1}{5} & \frac{1}{3} & 1 \end{bmatrix}$$
, The weight vector

derived from this matrix is (0.637,0.258,0.105).

Controlling Factors criterion (Well Pattern Control and Edge Water Energy), the pairwise comparison matrix is constructed as follows  $\begin{bmatrix} 1 & 2 \\ \frac{1}{2} & 1 \end{bmatrix}$ , The weight vector derived from this matrix is (0.667,0.333).

Development Potential criterion (Remaining Reserves and Water Cut), the pairwise comparison matrix is constructed as follows  $\begin{bmatrix} 1 & 5 \\ \frac{1}{5} & 1 \end{bmatrix}$ , The weight vector derived from this matrix is (0.833,0.167).

Based on the methodology described above, the comprehensive importance weight vector for the multi-factor evaluation of sand body development potential is derived as follows table 2.

Table 2 Multi-Factor Comprehensive Evaluation Importance Weight Vector

Evaluation Indicators	weight vector
Reserves	0.465
Area	0.188
Formation Coefficient	0.077
Well Pattern Control	0.126
Edge Water Energy	0.063
Remaining Reserves	0.067
Water Cut	0.014

After establishing the comprehensive indicator representation formula for the sand body, it is necessary to determine the evaluation value of each indicator, i.e., the degree of membership, in order to construct the evaluation matrix.

By applying either, a positive-oriented membership function or a negative-oriented membership function, each indicator is transformed into a comparable numerical value within a unified specified range shown in table 3.

Table 3 Membership Degree Values of Indicators for Each Sand Body

Catalogue	Horizon	Reserves	Area	Formation Coefficient	Well Pattern Control	Edge Water Energy	Remaining Reserves	Water Cut
Perforated Zones	s212	0.701	0.761	0.587	0.383	1.000	0.876	0.112
	s215	0.135	0.269	0.172	0.786	0.500	0.134	0.072
	s221	0.633	1.000	0.197	0.957	0.500	0.816	0.159
	s222	0.135	0.269	0.063	0.411	0.500	0.124	0.096
	s224	0.450	0.597	0.538	1.000	0.500	0.457	0.119
	s231	1.000	0.910	1.000	0.830	1.000	1.000	0.117
	s232	0.303	0.657	0.138	0.229	0.000	0.481	0.205
	s233	0.622	0.716	0.504	0.315	1.000	0.568	0.076
	s262	0.056	0.149	0.145	1.000	0.500	0.078	0.117
	s271	0.394	0.522	0.490	0.598	0.500	0.422	0.209
	s272	0.502	1.000	0.201	0.000	1.000	0.628	0.149
	s273	0.765	0.716	0.601	0.257	1.000	0.920	0.031
	s281	0.339	0.507	0.387	0.886	0.500	0.452	0.589
	s282	0.323	0.597	0.321	0.771	1.000	0.347	0.209
	s285	0.203	0.358	0.291	0.093	1.000	0.223	0.000
Non-Perforated Zones	s211	0.000	0.000	0.000	0.000	0.000	0.000	0.076
	s213	0.036	0.030	0.172	0.000	0.000	0.034	0.094
	s214	0.315	0.642	0.174	0.000	0.500	0.547	0.746
	s225	0.060	0.090	0.146	0.000	0.500	0.081	0.104
	s234	0.542	0.672	0.351	0.000	1.000	0.703	0.231
	s241	0.355	0.373	0.710	0.000	1.000	0.601	0.286
	s265	0.235	0.343	0.851	0.000	0.000	0.345	1.000
	s287	0.056	0.060	0.160	0.000	1.000	0.061	0.098

Based on the product of the membership degrees of indicators at all levels within the comprehensive evaluation weight vector for sand bodies, the comprehensive indicator value for each sand body was calculated through hierarchical computation. According to the distribution variation of these comprehensive indicator values, the sand bodies in the C1 Block were classified into three categories (Fig. 8).

Class I Sand Bodies exhibit a comprehensive indicator value ranging from 0.6 to 1.0. These sand bodies are characterized by relatively large reserves, with individual sand body reserves exceeding  $15 \times 10^4$ t, an oil-bearing area greater than  $0.5 \text{ km}^2$ , and an effective thickness of more than 2 m. They generally possess strong edge water energy, with current water cut mostly above 90% and a recovery factor typically exceeding 30%. This category includes 5 sand bodies, such as Es2<sup>31</sup> and Es2<sup>12</sup>.

Class II Sand Bodies have a comprehensive indicator value ranging from 0.3 to 0.6. These sand bodies display variable edge water energy: those with stronger edge water energy currently exhibit water cut mostly above 90% and a relatively high recovery factor, while those with weaker edge water energy show a lower recovery factor. This category comprises 9 sand bodies, including Es2<sup>24</sup> and Es2<sup>72</sup>.

Class III Sand Bodies yield a comprehensive indicator value in the range of 0.0 to 0.3. They are marked by smaller reserves, with individual sand body reserves below  $8 \times 10^4$ t, an oil-bearing area less than  $0.3 \text{ km}^2$ , and generally low formation coefficients. These sand bodies exhibit high water cut and a low recovery factor. This category includes 9 sand bodies, such as Es2<sup>15</sup> and Es2<sup>85</sup>.

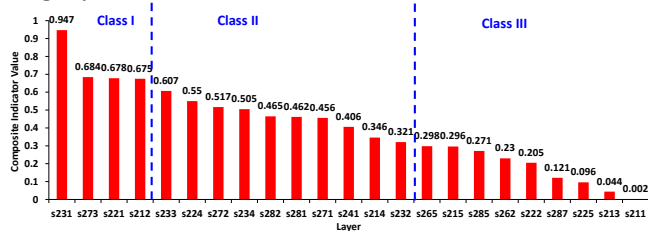


Fig8. Comprehensive Evaluation Scores and Classification of Sand Bodies

## 5. BASIS FOR ARTIFICIAL EDGE WATER FLOODING

### 5.1 Necessity of Artificial Edge Water Flooding

Artificial edge water flooding is a water injection technology recently proposed in the Shengli Oil Region. This technique involves large-well-spacing and high-rate water injection at the structurally low parts of complex fault-block reservoirs to simulate strong natural edge

water drive, thereby improving reservoir development performance. The key technical approach includes: Converting injection from the flank ("waist") to the periphery ("edge"); Increasing well spacing from narrow to large patterns; Shifting from controlled injection to intensified injection. After implementing artificial edge water flooding, the flow paths between injectors and producers change from a spindle-shaped pattern to a linear configuration.

In fault-block reservoirs with edge water shielded by faults, flank (waist) water injection causes tongue advancement, resulting in dispersed remaining oil in the flank areas and enriched accumulation in the high structural parts near faults. In contrast, artificial edge water drive promotes uniform flow path distribution, enabling even displacement within oil-bearing strips.

Taking the Es2<sup>33</sup> reservoir as an example, three well patterns under different drive mechanisms were designed to maximize the utilization of existing wells based on field conditions. The producing wells remained identical across all three scenarios. The injection strategies varied as follows: ① Natural Edge Water Drive: No injection wells were deployed, relying solely on natural aquifer support. ② Flank (Waist) Water Injection: Injection wells were placed in the mid-section of the oil layer to implement internal flooding. ③ Artificial Edge Water Injection: Injection wells were positioned beyond the oil-water boundary to simulate artificial edge water drive (Fig. 9).

Under equivalent fluid production rates and constant injection-production ratios, the performance of the three drive mechanisms was compared. The peripheral water injection scheme resulted in larger injector-producer spacing, improved sweep efficiency, and more uniform displacement. After 15 years of production, the cumulative oil production was highest under the peripheral water injection scenario. The recovery factors after 15 years for each mechanism were: Natural edge water drive: 10.13%, Flank water injection: 11.64%, artificial edge water injection: 13.02%. These results demonstrate that artificial edge water injection, which mimics natural edge water drive, is the optimal development strategy for fault-block reservoirs with edge water influence.

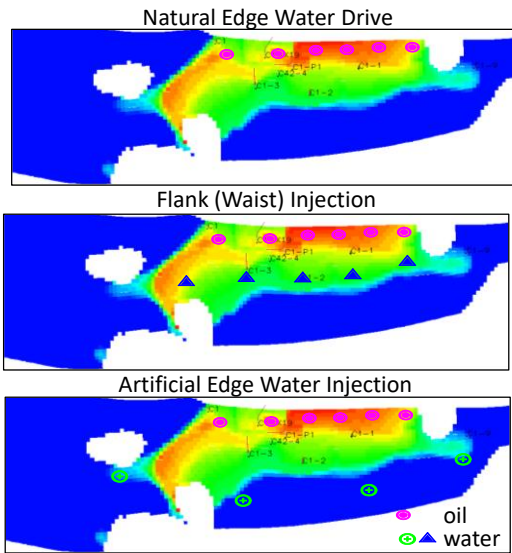


Fig9. Comparison of Different Well Patterns

## 5.2 Parameter Optimization

### 5.2.1 Optimization of Well Pattern Configuration

Reservoir in the C1 well area exhibits diverse structural characteristics across its sand groups: Sand Groups 1–4 form a fault-nose edge-water reservoir, Sand Groups 5–8 constitute a faulted anticline edge-water reservoir. Due to differences in edge-water distribution and remaining oil enrichment patterns between these reservoir types, well pattern designs must be customized accordingly. Thus, the well Pattern Strategy based on edge-water dynamics and remaining oil concentration, two linear well patterns were evaluated: staggered linear pattern and directly aligned linear pattern. (Fig.10) The staggered linear pattern recovery factor at the 15-year stage is 10.97%, whereas the directly aligned linear pattern is 9.53%. The staggered linear pattern demonstrated superior performance.

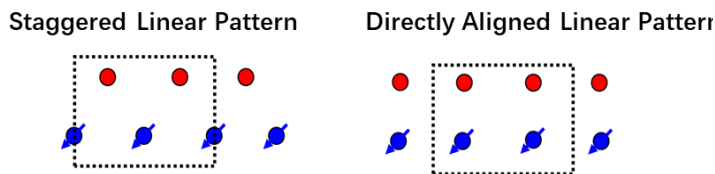


Fig10. Schematic Diagrams of Well Patterns

### 5.2.2 Optimization of Injection Strategy

Based on the design of staggered linear injection patterns, three distinct injection modes were analyzed (Fig.11). ① Staggered Linear Injection (Injectors and producers are arranged in a alternating pattern to promote uniform sweep) . The recovery factor at the 15-

year stage is 12.9%. ② Sparse Staggered Injection (A reduced-density variant of the staggered pattern, aiming to optimize well efficiency and reduce interference) .The recovery factor at the 15-year stage is 12.1%. ③ Alternating Staggered Injection (Injectors in the staggered pattern are divided into two groups (e.g. Group 1 Injectors is 1, 3, 5; Group 2 Injectors is 2,4))These groups alternate injection cycles to dynamically redistribute flow paths and enhance areal sweep. The recovery factor at the 15-year stage is 13.5%.

Optimization results shows that the alternating staggered injection mode demonstrated superior performance by effectively redirecting flow trajectories in the horizontal plane, expanding sweep coverage, and improving displacement efficiency. This approach proves most effective in maximizing reservoir contact and recovery.

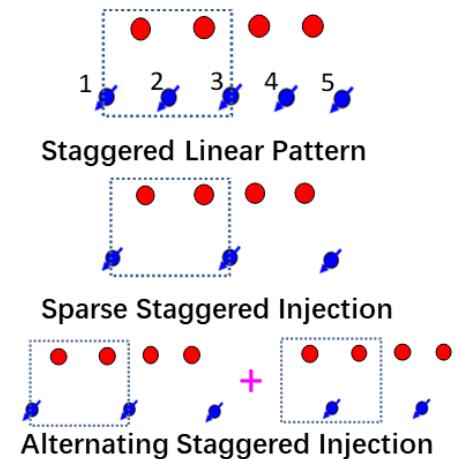


Fig11. Schematic Diagrams of Injection Strategy

### 5.2.3 Optimization of Alternating Injection Cycle

To determine the optimal alternating injection cycle, five scenarios with cycle lengths of 1, 2, 3, 4, and 5 years were designed. The performance of each scenario was assessed based on cumulative oil production over a 15-year development period.

The scenario with a 3-year alternating cycle yielded the highest cumulative oil production at the end of the 15-year period, demonstrating superior efficiency in enhancing sweep coverage and maximizing recovery. A 3-year alternating injection cycle is recommended to optimize development performance in the target reservoir (Fig.12).

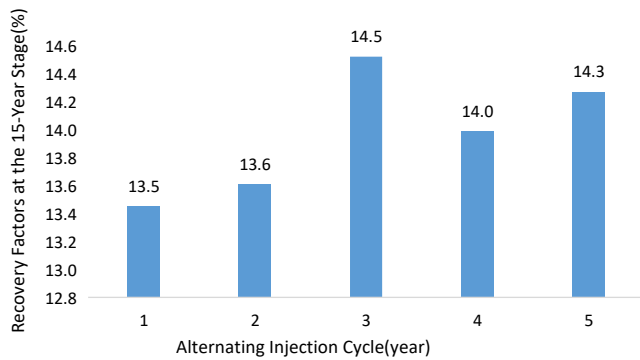


Fig12. Comparison of Recovery Factors at the 15-Year Stage Under Different Alternating Injection Cycles

#### 5.2.4 Optimization of Liquid Production Intensity

Based on field operational requirements, six scenarios with single-well liquid production rates of 10 m<sup>3</sup>/d, 20 m<sup>3</sup>/d, 30 m<sup>3</sup>/d, 40 m<sup>3</sup>/d, 50 m<sup>3</sup>/d, and 60 m<sup>3</sup>/d were designed. Numerical simulation was employed to predict the recovery factor under each production rate at the end of a 15-year development period. The simulation results indicate that higher liquid production rates correspond to increased recovery factors.

However, the incremental gain in recovery per additional 10 m<sup>3</sup>/d of liquid production is most significant above an average single-well rate of 20 m<sup>3</sup>/d (Fig.13).

To achieve a substantial improvement in recovery efficiency, it is recommended to maintain a liquid production intensity of no less than 25 m<sup>3</sup>/d. This strategy ensures a more effective increase in recovery while considering operational feasibility and reservoir response.

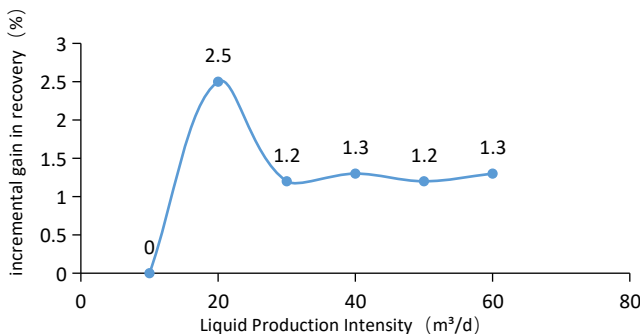


Fig13. Relationship Between Liquid Production Increase and Recovery Factor Increment

#### 5.2.5 Optimization of Injection-Production Ratio

In accordance with the injection capacity of water wells under field conditions, seven injection-production ratio scenarios were designed: 0.5, 0.8, 1.0, 1.2, 1.3, 1.4,

and 1.5. The simulation results demonstrate that cumulative oil production over a 15-year development period increases significantly when the injection-production ratio exceeds 1.4. Above this threshold, the incremental gain in production becomes more pronounced (Fig.14).

To achieve enhanced development performance, it is recommended to maintain an injection-production ratio of no less than 1.4. This strategy ensures more effective pressure maintenance and improved sweep efficiency, thereby maximizing long-term recovery.

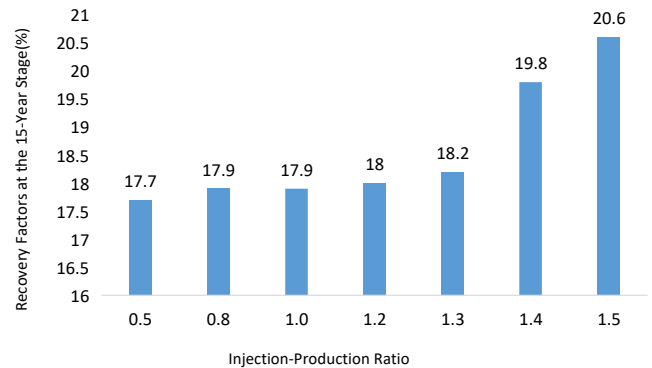


Fig14. Comparison of Recovery Factors at the 15-Year Stage Under Different Injection-Production Ratio

## 6. IMPLEMENTATION RESULTS

Based on the layer-series reclassification and reorganization in the C1 Block, an artificial intensified edge-water flooding development adjustment plan was formulated and implemented. The planned engineering activities have been completed, yielding significant improvements in development performance.

As of the latest assessment, the following results have been achieved: 7 new wells have been put into production, contributing a cumulative oil production of 5.8 thousand tons; 10 existing wells have been adjusted through layer-series reallocation, resulting in a cumulative incremental oil production of 3.6 thousand tons; 2 wells have been converted to water injection, providing a cumulative additional water injection volume of 4.5 thousand cubic meters; The block's daily oil production has increased from 56 t/d before implementation to the current 89 t/d; The natural decline rate has been reduced by 1.5%; The oil recovery rate has improved by 0.12%. These outcomes demonstrate a substantial enhancement in the overall development efficiency of the block.

## 7. CONCLUSIONS

Low-amplitude structures exert significant control over the original distribution and enrichment of hydrocarbons in the C1 Block reservoir. These structures serve as favorable pathways for hydrocarbon migration and relatively enriched accumulation areas. As the structural amplitude increases and the structural position rises, the reservoir thickness increases, well productivity gradually improves, water cut decreases, and the rate of water cut rise slows. The spatial extent of this control and influence varies systematically with the undulations of the low-amplitude structures.

Severe inter-layer interference occurs when inter-layer heterogeneity is pronounced, leading to uneven water absorption across sub-layers in injection wells and significant differences in average remaining oil saturation and comprehensive water cut among layers. This necessitates subdivision and reorganization of the layer series. The single-layer development strategy in the C1 Block cannot simultaneously address both main and non-main layers effectively.

Low-amplitude structural reservoirs are characterized by insufficient natural aquifer support and rapid water cut rise. Remaining oil is primarily concentrated in structural highs. By re-configuring flood fronts and implementing an artificial edge-water flooding development mode, both the oil production rate and ultimate recovery can be enhanced.

## REFERENCE

- [1] Zhilin, W. , Bo, L. , Yongtao, G. E. , Fulai, Y. , Xiaonan, L. I. , & Amp, E. , et al. (2019). Mechanisms and optimization of supplementing in-situ energy by co<sub>2</sub> injection after water flooding in low permeability reservoirs. *Fault-Block Oil & Gas Field*.
- [2] Zhi-Wei, W. U. . (2017). Experimental research and potential evaluation about remaining oil distribution after water flooding in heterogeneous reservoir. *Science Technology and Engineering*.
- [3] Caineng, Z. , Shizhen, T. , Xuanjun, Y. , Rukai, Z. , Dazhong, D. , & Wei, L. , et al. (2009). Global importance of "continuous" petroleum reservoirs: accumulation, distribution and evaluation. *Petroleum Exploration & Development*, 36(6), 669-682.
- [4] Chao-Lia, L. , Jun-Feng, Z. , Ming-Huib, Y. , & Jin-Xiub, W. . (2010). Characteristics and formation mechanism of low-relief structural-lithological reservoir with edge and bottom water:a case from the sai 152 pool,ordos basin. *Geological Science and Technology Information*, 29(4), 78-83.
- [5] Yong-Gang, W. , Zhi-Gang, W. , & Ling, C. . (2009). Study on water-flooding influential factors in super-low permeability reservoirs——by taking chang 8 reservoir of middle baima area in xifeng oilfield as an example. *Journal of Oil and Gas Technology*.
- [6] Ji-Xiang, L. I. , Hong-Tao, H. , Li, Z. , Bo, T. , & Mei-Li, M. . (2011). Research on block-removal and injection stimulation technology for water injectors in low permeability reservoirs. *Special Oil & Gas Reservoirs*.
- [7] Shu-Yun, W. U. , & Jing-Tao, Z. . (2005). Practice and acknowledgment on shallow profile modification in gaotaizi reservoirs in sazhong area. *Petroleum Geology & Oilfield Development in Daqing*.
- [8] Peng, L. , Han, J. , Zhen, J. , & Guo, Z. . (2009). Adaptability of water flooding with horizontal wells in low permeability reservoirs. *Special Oil & Gas Reservoirs*.
- [9] Jianmin, W. , San, Z. , Wei, D. U. , Le, L. I. , Zhen, Q. , & Jun, Z. , et al. (2019). The control effect of low-amplitude structure on oil-gaswater enrichment and development performance of ultra-low permeability reservoirs. *Petroleum Exploration and Development*(4).
- [10] Yan, J. , Zhang, N. S. , & Liu, X. J. . (2008). Study on the stimulation mechanism of the advanced water flooding in low-permeability oilfield. *Journal of Xi'an Shiyou University(Natural Science Edition)*.
- [11] Wei, J. , Zhang, D. , Zhang, X. , Zhao, X. , & Zhou, R. . (2023). Experimental study on water flooding mechanism in low permeability oil reservoirs based on nuclear magnetic resonance technology. *Energy*, 278.
- [12] Yuan, W. , Hou, J. , Yang, Y. , Zhao, Y. , & Nie, H. . (2023). Experimental study on nano polymer microspheres assisted low salinity water flooding in low permeability reservoirs. *SPE 217284-MS.2023*
- [13] Zhou, Q. , Jiang, H. Q. , & Chen, M. F. . (2008). Fracturing parameter optimization of the water wells in low-permeability reservoirs. *Journal of Xi'an Shiyou University(Natural Science Edition)*.